Acta Crystallographica Section D
Biological Crystallography
ISSN 0907-4449

Tobacco uroporphyrinogen-III decarboxylase: characterization, crystallization and preliminary X-ray analysis

Berta M. Martins,[a]* Bernhard Grimm,[b,c] Hans-Peter Mock,[c] Gerald Richter,[d] Robert Huber[a] and Albrecht Messerschmidt[a]

[a]Max-Planck-Institut für Biochemie, Abt. Strukturforschung, Am Klopferspitz 18-a, D-82152 Martinsried bei München, Germany, [b]Lehrstuhl für Pflanzenphysiologie, Humbolt Universität zu Berlin, Unter den Linden 6, D-10099 Berlin, Germany, [c]Institut für Pflanzengenetik und Kulturpflanzenforschung, Abt. Molekulare Zellbiologie, Correnstrasse 3, D-06466 Gatersleben, Germany, and [d]Technische Universität München, Abt. Organische Chemie und Biochemie, Lichtenbergstrasse 4, D-85748 Garching, Germany

Correspondence e-mail: martins@biochem.mpg.de

Received 13 July 2001
Accepted 10 August 2001

Uroporphyrinogen-III decarboxylase from *Nicotiana tabacum* is a plastidial enzyme involved in the biosynthesis of chlorophyll and haem. Sedimentation equilibrium with protein producing diffracting crystals clearly indicates that the enzyme is a homodimer under similar ionic strength conditions to those found in the chloroplast stroma. Additionally, dynamic light scattering reveals an ionic strength dependence for this oligomerization state. Crystals were obtained in the hexagonal space group *P*622 with one molecule per asymmetric unit and diffracted to 2.3 Å resolution using synchrotron radiation.

1. Introduction

The tetrapyrrole biosynthetic pathway provides several prosthetic groups and cofactors supporting the enzymatic catalysis of natural biological processes. All these tetrapyrrole-based molecules share a common macrocyclic precursor, uroporphyrinogen-III (uro-III). In the biosynthesis of chlorophyll and haem, the multi-step decarboxylation of uro-III to produce coproporphyrinogen-III is solely catalysed by uroporphyrinogen-III decarboxylase (UROD; E.C. 4.1.1.37), with no apparent requirement for prosthetic groups or cofactors (de Verneuil *et al.*, 1983; Straka & Kushner, 1983). The UROD amino-acid sequence has been well conserved throughout evolution with an overall similarity of 33% and two unique signature patterns (Prosite documentation access number PDOC00705; Garey *et al.*, 1992). Whereas plant UROD is found in the plastids, in mammals, yeast and some bacteria it is cytosolic (Jacobs & Jacobs, 1993).

Extensive biochemical and site-directed mutagenesis studies have allowed the identification of several putative functional side chains (Kawanishi *et al.*, 1983; de Verneuil *et al.*, 1983; Straka & Kushner, 1983; Felix & Brouillet, 1990; Wyckoff *et al.*, 1996). Recently, the three-dimensional structure of the homologous protein from human (Whitby *et al.*, 1998) confirmed the presence of one sole active cleft per molecule (Elder & Roberts, 1995) and the crystallographic dimer suggested a putative interaction between catalytic clefts of the two monomers. However, the sequence of protein substrate interactions during the catalysis remains unknown. In order to understand how UROD performs its unique multi-decarboxylation reaction, more structural information is needed.

In parallel to its enormous economic impact on agriculture and biotechnology owing to its potential application in the design of environmentally safe herbicides, research on the enzymes involved in the tetrapyrrole metabolism in plants can contribute to the development of effective treatments for porphyrias. The present work reports the characterization of the recombinant mature tobacco UROD and its crystallization alone and in the presence of inhibitors.

2. Experimental

2.1. Characterization of purified tobacco UROD

The recombinant mature tobacco UROD (39 kDa) was expressed and purified as described elsewhere (Mock *et al.*, 1995). N-terminal peptide sequencing and SDS–PAGE (10–12.5%) assessed its integrity and purity. The protein concentration was determined by absorption spectroscopy using a molar extinction coefficient (at 280 nm) of 35 590 M^{-1} cm^{-1}.

The oligomerization state in solution was analysed by dynamic light scattering (DLS) and sedimentation equilibrium. DLS analysis was performed at 293 K using a DynaPro-801TC (Protein Solutions, Charlottesville, USA). Protein samples at 2–5 mg ml^{-1} in 10 m*M* Tris–HCl pH 7 (buffer *A*) and buffer *A* with 50 m*M* $(NH_4)_2SO_4$ were filtered according to the manufacture's instructions and 20–25 readings were taken per sample.

For sedimentation equilibrium, the protein was diluted to an optical density of 0.3 at 280 nm in 50 m*M* Tris–HCl pH 7.5, 100 m*M* NaCl. Samples were spun to equilibrium in a Beckman Optima XL-I analytical ultra-

Table 1
Dynamic light-scattering data.

Protein buffer	Hydrodynamic radius (nm)	Polydispersity index	Estimated MW (kDa)
Buffer *A*	3.43	0.07	57.4
Buffer *A* + 50 m*M* $(NH_4)_2SO_4$	3.95	0.1	81.2

centrifuge at 293 K. The partial specific volume of the protein and the density of the solvent were estimated according to published procedures (Lane *et al.*, 1992).

2.2. Crystallization and X-ray data collection

Prior to crystallization, the protein was concentrated to approximately 5 mg ml^{-1} using a Centricon concentrator (30 kDa cutoff) in buffer *A*. The initial crystallization trials were carried out with a grid screen of $(NH_4)_2SO_4$ *versus* pH 9–12 (solutions buffered with 250 m*M* sodium borate/boric acid). The droplets were made by mixing 3 µl of protein solution with 1 µl of reservoir solution (1 ml) using the hanging-drop vapour-diffusion method at 295 K. When combining a diluted protein with a double drop volume, small crystals were obtained in 1.2 *M* $(NH_4)_2SO_4$ at pH 9.6, reaching dimensions of roughly 400 × 250 × 50 µm after 18 months. The diffraction quality of the crystals was tested on an in-house imaging-plate detector (MAR Research, Germany) coupled to a Rigaku RU-200 rotating-anode X-ray generator (Tokyo, Japan) producing Cu $K\alpha$ radiation with a wavelength of 1.5418 Å.

For data collection using synchrotron radiation, the crystals were harvested with cryoloops of the same dimensions, briefly immersed in cryoprotectant buffer [1.5 *M* $(NH_4)_2SO_4$, 100 m*M* MOPS pH 7.5, 10%(*v*/*v*) 2,3-*R*,*R*-butanodiol] and flash-cooled in a nitrogen stream at 100 K (using an Oxford Cryosystems Cryostream, England).

Co-crystallization trials in the presence of inhibitors (uroporphyrin-III, coproporphyrin-III and mesoporphyrin-IX, purchased from Porphyrin Products, Logan, USA) were performed by adding 0.1 µl from inhibitor solutions (10–100 µ*M*) to the droplets. For soaking experiments, crystals were transferred into pre-equilibrated droplets containing one of the inhibitors at 10 µ*M*. To avoid photoactivation of these porphyrins, all trials were kept in the dark.

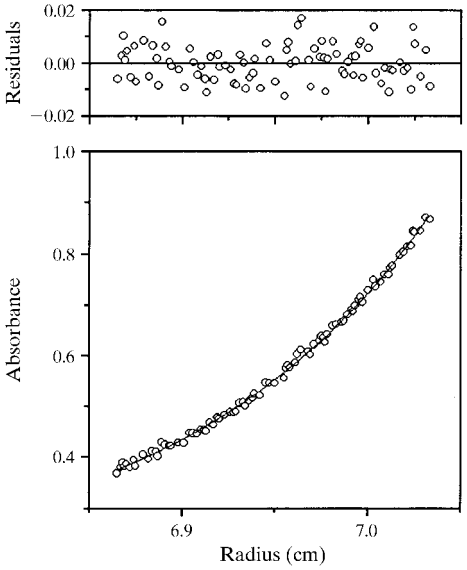

Figure 1
Sedimentation equilibrium of tobacco UROD. Conditions used were 10 000 rev min^{-1} and 295 K.

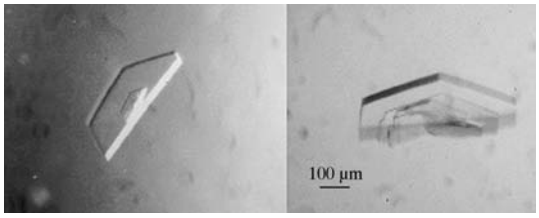

Figure 2
Crystal of tobacco UROD grown from 1.2 *M* $(NH_4)_2SO_4$ pH 9.6 at 295 K.

3. Results and discussion

The availability of a reasonable amount of protein with a high degree of purity and molecular homogeneity is essential for crystallization purposes. The purity of the recombinant tobacco UROD was assessed by SDS–PAGE, which showed the presence of a single band corresponding to the molecular weight of the mature protein; the correct N-terminal amino-acid sequence (VAEPKA) was confirmed by N-terminal peptide sequencing.

Sedimentation equilibrium and DLS experiments were performed to verify the oligomerization and the monodispersity of the enzyme. Sedimentation-velocity analysis showed that the protein sediments as a single symmetrical boundary with a velocity of 4.0 S (data not shown). Sedimentation equilibrium data could be fitted by a single exponential, suggesting ideal solute behaviour under the conditions used. The fitted line in Fig. 1 was calculated for a mass of 82 kDa. Residuals indicating the close agreement between the theoretical curves and the experimental data are shown in the upper part of the figure. This clearly indicates that tobacco UROD is a homodimer under similar ionic strength conditions to those found in the chloroplast stroma (Neuhaus & Wagner, 2000). DLS revealed an ionic strength dependence for this dimerization. Whereas in buffer *A* the calculated molecular weight is 1.5 times that of the monomer, it corresponds to the dimer mass in the presence of the crystallization precipitant $(NH_4)_2SO_4$. Table 1 summarizes these results.

Based on the calculated isoelectric point of the protein (pI 9.4), the initial crystallization trials were performed varying the concentration of $(NH_4)_2SO_4$ *versus* a pH range around this pI value. Crystals were obtained as indicated in §2.2 and shown in Fig. 2. In addition to their poor diffraction quality, the crystals were very sensitive to radiation, preventing the collection of complete data sets from single crystals at room temperature.

The search for a cryoprotectant solution based on the crystallization solution gave no results and only the combination of a new buffer composition together with an increase in the salt concentration made it possible to flash-cool the crystals. Even so, the crystals had to be rapidly passed through the cryoprotectant solution, which was difficult to reproduce and resulted in the destruction of a large number of crystals. The breakthrough came from pre-equilibrating the cryoprotectant solution in air (5–10 min) prior to immersion of crystals. Upon cooling in a nitrogen stream (100 K) the crystals diffracted to 2.3 Å using synchrotron radiation (Fig. 3). The crystals belong to space group *P*622, with unit-cell parameters $a = b = 158.44$, $c = 67.68$ Å. The

Table 2
Data-collection statistics.

Values in parentheses refer to the outer resolution shell.

Resolution range (Å)	18.0–2.30 (2.34–2.30)
Collected reflections	47385
Unique reflections	22173
Completeness (%)	97.7 (98.3)
R_{sym}† (%)	6.0 (34.6)
$I/\sigma(I)$	26.1 (4.3)

† $R_{sym} = \sum |I - \langle I \rangle| / \sum \langle I \rangle$, where $\langle I \rangle$ is the average intensity for multiple observations of symmetry-related reflections.

crystal unit cell has a solvent content of 61% (V_M = 3.14 Å^3 Da^{-1}; Matthews, 1968), corresponding to one molecule per asymmetric unit. The high solvent content may account for the crystal instability when directly exposed to the X-rays. A complete data set was collected from a single crystal using a MAR CCD detector on wiggler beamline BW6 (DESY, Germany) using synchrotron radiation with a wavelength of 1.05 Å. Data were evaluated using *DENZO* and *SCALEPACK* (Otwinowski & Minor, 1996) (Table 2).

Figure 3
Diffraction pattern of tobacco UROD. The resolution at the edge of the image is 2.3 Å.

Co-crystallization experiments only produced crystals in the presence of uroporphyrin-III. Although displaying a similar habit, the crystal nucleation seemed to be slower (~2–3 months for the first optical detection). Additionally, the crystals stop growing after reaching dimensions of roughly 100 × 100 × 20 µm, which most probably explains the weak diffraction observed under cryoprotectant conditions (8–6 Å). All soaking experiments resulted in destruction of the crystals. Work is in progress to improve cocrystallization conditions.

The availability of the three-dimensional structure for the homologous human protein (Whitby *et al.*, 1998) will enable the use of Patterson search methods to determine the crystal structure from tobacco UROD.

This work was supported in part by a fellowship PRAXIS XXI BD/9656/96 (to BMM) from the Fundação para a Ciência e a Tecnologia, Portugal. G. P. Bourenkov (DESY, Germany) is gratefully acknowledged for help with synchrotron data collection and U. Jacob for helpful discussions.

References

Elder, G. H. & Roberts, A. G. (1995). *J. Bioenerg. Biomembr.*, **27**, 207–214.
Felix, F. & Brouillet, N. (1990). *Eur. J. Biochem.* **188**, 393–403.
Garey, J. R., Labbe-Bois, R., Chelstowska, A., Rytka, J., Harrison, L., Kushner, J., & Labbe, P. (1992). *Eur. J. Biochem.* **205**, 1011–1016.
Jacobs, J. M. & Jacobs, N. J. (1993). *Plant Physiol* **101**, 1181–1187.
Kawanishi, S., Seki, Y. & Sano, S. (1983). *J. Biol. Chem.* **258**, 4285–4292.
Lane, T. M., Shah, B. D., Ridgeway, T. M. & Pelletier, S. L. (1992). *Analytical Ultracentrifugation in Biochemistry and Polymer Science*, edited by S. E. Harding, A. J. Rowe & A. J. Horton, pp. 90–125. Cambridge: Royal Society of Chemistry.
Matthews, B. W. (1968). *J. Mol. Biol.* **33**, 491–497.
Mock, H. P., Trainotti, L., Kruse, E. & Grimm, B. (1995). *Plant Mol. Biol.* **28**, 245–256.
Neuhaus, H. E. & Wagner, R. (2000). *Biochim. Biophys. Acta*, **1465**, 307–323.
Otwinowski, Z. & Minor, W. (1996). *Methods Enzymol.* **276**, 307–326.
Straka, J. G. & Kushner, J. P. (1983). *Biochemistry*, **22**, 4664–4672.
Verneuil, H. de, Sassa, S. & Kappas, A. (1983). *J. Biol. Chem.* **258**, 2454–2460.
Whitby, F. G., Phillips, J. D., Kushner, J. P. & Hill, C. P. (1998). *EMBO J.* **17**, 2463–2471.
Wyckoff, E. E., Phillips, J. D., Sowa, A. M., Franklin, M. R. & Kushner, J. P. (1996). *Biochim. Biophys. Acta*, **1298**, 294–304.